PCCP

Accepted Manuscript


This is an *Accepted Manuscript*, which has been through the Royal Society of Chemistry peer review process and has been accepted for publication.

*Accepted Manuscripts* are published online shortly after acceptance, before technical editing, formatting and proof reading. Using this free service, authors can make their results available to the community, in citable form, before we publish the edited article. We will replace this *Accepted Manuscript* with the edited and formatted *Advance Article* as soon as it is available.

You can find more information about *Accepted Manuscripts* in the Information for Authors.

Please note that technical editing may introduce minor changes to the text and/or graphics, which may alter content. The journal's standard Terms & Conditions and the Ethical guidelines still apply. In no event shall the Royal Society of Chemistry be held responsible for any errors or omissions in this *Accepted Manuscript* or any consequences arising from the use of any information it contains.

ROYAL SOCIETY OF CHEMISTRY

www.rsc.org/pccp

Journal Name

RSCPublishing

COMMUNICATION

# Facile fabrication of Porous CL-20 for Low Sensitivity High Explosives

Cite this: DOI: 10.1039/xoxxoooooox

Jinpeng Shen,[a,c] Weimei Shi, [a,c] Jun Wang, [a] Bing Gao, [b] Zhiqiang Qiao, [a] Hui Huang, [a] Fude Nie,[a] Rui Li, [a,c] Zhaoqian Li, [b] Yu Liu, [a] and Guangcheng Yang,*[a,c]

Received ooth January 2012,
Accepted ooth January 2012

DOI: 10.1039/xoxxoooooox

www.rsc.org/

**A facile solvent/non-solvent co-crystallization technology is applied to fabricate porous CL-20, which exhibits interesting morphologies and low sensitivity with β-cyclodextrin as a crystal modifier.**

The self-assembly of micro- and nanostructures is a facile and efficient method for controlling the structure of porous materials. This method has elicited considerable attention because porous materials often exhibit outstanding properties because of their micro- and nanostructures [1] and have found various applications in catalysis, adsorption, separation, sensing, and biotechnology to date.[2]

Nowadays, CL-20 (2,4,6,8,10,12-hexanitro-2,4,6,8,10,12-hexaazaisowurtzitane),[3] which is a typical high explosive with cage structure, has been one of the most powerful explosives that have drawn much interest because of their potential application in propellants and military fields.[4] CL-20 has five polymorphs (α, β, γ, ε, and ζ). Several factors such as recrystallization method and the solvent influence the crystal type, which determine the phase being produced. However, drawbacks, such as high sensitivity to external stimuli, shock, friction, and flame, have limited the industrial application of CL-20. In this study, we attempted to design a new porous structure by integrating self-assembly with crystal engineering technology to preserve high energy and reduce sensitivity. A promising approach known as solvent/non-solvent (S/NS) co-crystallization[5] uses organic additives and/or templates by controlling the nucleation and growth and by forming porous materials from molecule to crystal.[6] Crystal engineering technology is also one of the most important methods for understanding the intermolecular interactions of crystal packing and the design of new materials with desired physical and chemical properties.[7] Beta-cyclodextrin (β-CD) is selected as a crystal modifier because of its significance in self-assembly and crystal engineering.[8] β-CD is also easy to remove by washing in running water.

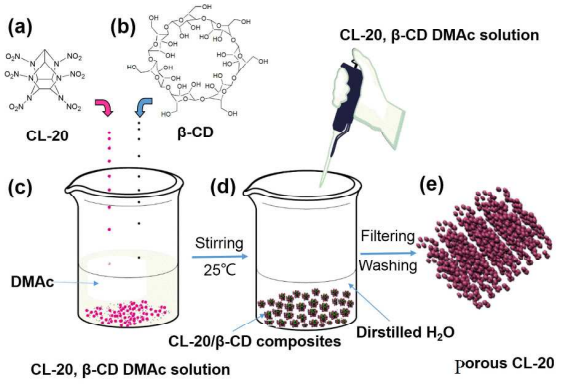


Fig. 1 Schematic S/NS co-crystallization method of preparing porous-CL20, (a) CL-20 ($C_6H_6N_{12}O_{12}$), (b) β-CD ($C_{42}H_{70}O_{35}$), (c) CL-20, β-CD and DMAc solution, (d) co-crystallization of CL-20 and β-CD, and (e) schematic of porous-CL20.

In this study, we report a facile S/NS co-crystallization method for synthesizing low-sensitivity porous CL-20 in contrast to ε-CL-20 with β-CD as a crystal modifier. A possible formation process of porous CL-20 during

Physical Chemistry Chemical Physics Accepted Manuscript

the crystallization process of CL-20 is proposed via experimental and molecular dynamics (MD) simulation. Fig. 1 shows the schematic of the porous CL-20 preparation. The use of β-CD as a crystal modifier for controlling the nucleation, growth, and alignment of CL-20 molecules could be a promising strategy. More importantly, the whole preparation process of CL-20 is performed in the solution, thereby ensuring safety.

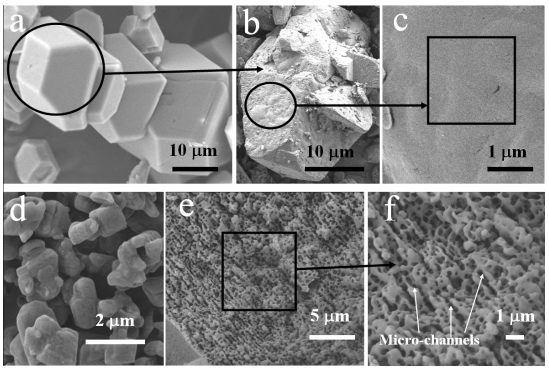


Fig. 2 SEM of (a) ε-CL20 crystal, (b) internal surface of ε-CL20 crystal, (c) magnification of a part of (b), (d) CL-20 of recrystallization without β-CD, (e) cross-section view of porous CL-20, and (f) magnification of cross-section view.

Fig. 2 shows the typical scanning electron microscopy (SEM, FEI-Nova NanoSEM600) images of ε-CL-20 (Figs. 2a–2c), CL-20 of recrystallization without β-CD (Fig. 2 d), and porous CL-20 (Figs. 2e and 2f) crystals. Figs. 2a and 2b reveal the morphological characteristics of ε-CL-20 crystal with a prismatic microstructure and particle size of 10 μm to 40 μm (Fig. 2a) as well as the internal surface of the ε-CL-20 crystal (Fig. 2b). Fig. 2c shows the magnification of the internal surface of the ε-CL-20 crystal. The surface and inside of the ε-CL-20 crystal do not have tiny holes (Figs. 2a–2c). Interestingly, a kind of porous CL-20 (Fig. 2e) was fabricated via S/NS co-crystallization method with β-CD as a crystal modifier. Several tiny holes with a mean pore diameter of 500 nm are observed on the cross-section. These holes also form many microchannels (Fig. 2f) in one direction (more details are shown in ESI, Fig. S1). The porous CL-20 had a Brunauer–Emmett–Teller surface area of 5.5 $m^2/g$ and pore sizes of 5.9 and 17.7 nm (Fig. 3a). The XRD patterns also indicate that the porous CL-20 is the α-CL-20 crystal [Fig. 3b (1)], which is in agreement with the α-CL-20 [Fig. 3b (2)] from the Cambridge Structural Database (CSD, PDF2#: 00-052-2431). Fig. 3b (3) also shows that the crystal type of the raw material is ε-CL-20 (CSD, PDF2#: 00-050-2045). Fig. S2, Fig. S3, and Table S3 show the thermal behavior of porous CL-20 and ε-CL-20. For porous CL-20 and ε-CL-20, the solid–solid phase transition of α → γ and ε → γ is observed at about 159.2 °C and 152.5 °C, respectively. The exothermic decomposition peak of the porous CL-20 also reaches 232.3 °C and decreases by 3.3 °C compared with that of ε-CL-20 at 235.6 °C (Fig. S3).[9] More importantly, the decomposition enthalpy (ΔH = 1975.8 $J \cdot g^{-1}$) of porous CL-20 during the decomposition process is close to that of the ε-CL-20 (ΔH = 1980.3 $J \cdot g^{-1}$). This finding implies that excellent thermal behavior is maintained before and after microstructure change. In addition, the purity of porous CL-20 is 99.7%, which is in agreement with that of raw CL-20, as determined via high-performance liquid chromatography (HPLC). The results of impact sensitivity tests indicated that the $H_{50}$ value for the porous CL-20 is 49 cm. The $H_{50}$ values for ε-CL-20 and α-CL-20 are 21 and 19 cm, respectively (Table S4). Consequently, the higher value of $H_{50}$ indicates that the impact sensitivity of porous CL-20 was reduced. This finding can be attributed to the porous structure, which may disperse the shock forces that act on the explosives. The smart structure also prevents the formation of "hot spots" at which the chemical reaction was induced for explosion.

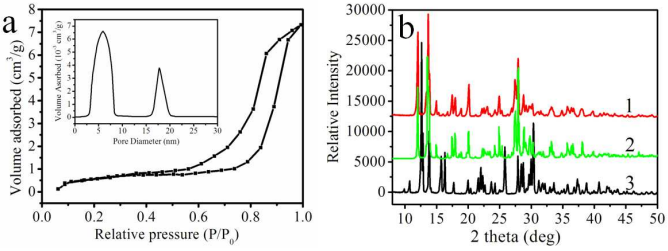


Fig. 3 (a) Adsorption isotherm and corresponding pore size distribution curve (inset) of porous CL-20 from BET, (b) XRD patterns of (1) porous CL-20, (2) α-CL-20 (Cambridge Structural Database, CSD: PDF2#: 00-052-2431), and (3) ε-CL-20 (CSD: PDF2#: 00-050-2045).

The excellent performance is significantly affected by the material structure. To further understand the self-assembly mechanism during porous CL-20 crystallization, grown facets were predicted via MD simulations. The experimental results indicate that a α-CL-20 crystal model was built. The grown facets were

Physical Chemistry Chemical Physics Accepted Manuscript


This journal is © The Royal Society of Chemistry 2012

predicted based on morphology with the attachment energy model in the Materials Studio 5.5 (more details in ESI). The compass force field and force field assigned charges were used in the prediction of grown facets (Table S1). Five main crystal grown facets were detected, namely, (0 0 2), (0 2 0), (1 0 2), (0 2 1), and (1 1 1). Among these facets, (0 0 2) has the largest total facet area. The length of $d_{hkl}$ follows the relationship $d_{(0\ 0\ 2)} > d_{(0\ 2\ 0)} > d_{(1\ 0\ 2)} > d_{(0\ 2\ 1)} > d_{(1\ 1\ 1)}$. According to the balance of crystal morphology theory,[10] the relation is $R \propto 1/d_{(hkl)} \propto h_{(hkl)}$ among the crystal face growth rate ($R$), the interplanar crystal distance ($d_{(hkl)}$), and the distance $h_{(hkl)}$ from crystal center to each crystal face. Therefore, the relative order of $R$ is $R_{(0\ 0\ 2)} < R_{(0\ 2\ 0)} < R_{(1\ 0\ 2)} < R_{(0\ 2\ 1)} < R_{(1\ 1\ 1)}$. The surface free energy of each crystal face is also directly proportional to its $h_{(hkl)}$ based on the Curie–Wulff theory.[11] Therefore, $R$ is proportional to the specific surface energy. The CL-20/β-CD composite model is most stable when the CL-20 molecule is substituted by β-CD on the surface (0 0 2) of CL-20 with the lowest surface free energy.

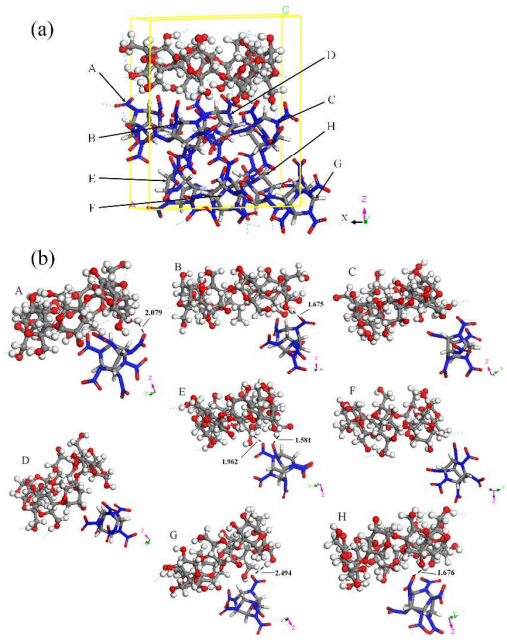


Fig. 4 MD simulations: (a) CL-20/β-CD composite model and (b) magnification of a part of the image shown in (a).

According to the growth facets prediction, the CL-20/β-CD crystal is built by cleaving the (002) facet, and then built a vacuum slab for 10 Å. There are eight CL-20 molecule in the crystal unit (CL-20 molecule is shown as stick-and-stick model), and add a β-CD molecular on the (002) facet (β-CD molecule is shown as ball-and-stick model) (Fig. 4a). The molar ratio of CL-20 and β-CD is 8:1 based on our experimental data. Abundant intermolecular hydrogen bonds (N-O · · · H) (Table S2) were detected between the CL-20 and β-CD molecules between -$NO_2$ (CL-20) and -OH (β-CD) (Fig. 4b).

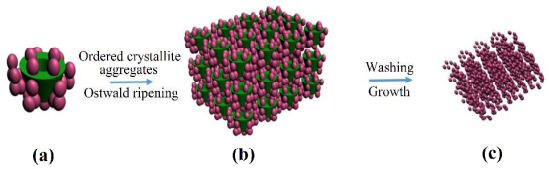


Fig. 5 Schematic of self-assembly process of porous CL-20: (a) growth of the crystal nucleation, (b) ordered crystallite aggregates, and (c) formation of porous and further growth.

Based on the above results, a three-step process is proposed for porous CL-20 formation (Fig. 5). (1) Nucleation: When the dimethylacetamide (DMAc) solution of CL-20 and β-CD was slowly poured into the distilled water, which is a non-solvent for CL-20 and β-CD, the DMAc solution was separated into small droplets. Each small droplet containing CL-20 and β-CD molecules was surrounded by a large volume of distilled water. Given the principle of DMAc solution in distilled water, these droplets quickly became supersaturated and provided critical sites for nucleation in phase transformations. Based on the CL-20/β-CD composite model (Fig. 4), abundant intermolecular hydrogen bonds were found within the cell, which also benefited the nucleation. (2) Ordered crystallite aggregates: Supersaturation can be the main driving force for continuing growth based on crystal nucleation. With increasing CL-20 and β-CD concentrations, the velocities of nucleation and crystal growth of CL-20/β-CD crystallites were also accelerated. Moreover, (0 0 2), which is one of the crystal grown facets, has the largest total facet area that contributed most to the orientated growth of CL-20/β-CD composites. The crystallite directly merged with their neighboring crystallite, which has a similar crystallographic orientation to minimize their interfacial energy through Ostwald ripening growth[12] in a solution environment, thereby resulting in 3D growth (Fig. 5b). (3) Formation of porous: β-CD was almost removed after washing the 3D CL-20/β-CD

Physical Chemistry Chemical Physics Accepted Manuscript

composites with a large volume of distilled water. This finding is ascribed to the difference in the solubilities of CL-20 and β-CD in distilled water. Given that β-CD exists in the crystallite aggregate process, the removal of β-CD would definitely result in porous CL-20 structure (Fig. 5c).

## Conclusions

In summary, a novel porous CL-20 was prepared via an efficient S/NS process with β-CD as a crystal modifier. The obtained porous CL-20 structure displays sufficiently reduced sensitivity in contrast to that of ε-CL-20. The $H_{50}$ value increased from 21 cm (ε-CL-20) to 49 cm (porous CL-20), which may be attributed to the porous structure. The decomposition enthalpy during the decomposition process had no significant difference before and after the microstructure change. We also proposed a possible formation process based on theoretical calculations and experimental results. This interesting porous structure offers new insights into preparation of other low sensitivity energetic materials.

## Acknowledgments

This work was supported by the National Natural Science Foundation of China (No.11272292,11372288)National High Technology Research and Development P rogram of China (863 Program) (No. 2013AA050905). Development Foundation of CAEP (No. 2014B0302041). Science Foundation for Young Scientist of Sichuan Province (2012JQ0038), and Young Talent Foundation of Institute of Chemical Materials (QNRC 2012-1 and QNRC 2013-10).

## Notes and references

[a] *Institute of Chemical Materials, China Academy of Engineering Physics, Mianyang 621900, Sichuan, China. E-mail: ygcheng@caep.cn; sjp0388@163.com; Tel: +86-08162544436; Fax: +86-08162544426*

[b] *State Key Laboratory Cultivation Base for Nonmetal Composites and Functional Materials, Southwest University of Science and Technology, Mianyang 621010, P. R. China.*

[c] *Sichuan New Material Research Center, Mianyang 621000, Sichuan, China.*

*†Electronic Supplementary Information (ESI) available: [details of any supplementary information available should be included here]. See DOI: 10.1039/b000000x/*

‡ Footnotes should appear here. These might include comments relevant to but not central to the matter under discussion, limited experimental and spectral data, and crystallographic data.

1 M. E. Davis, *Nature*, 2002, **417**, 813; J. Y. Ying, C. P. Mehnert and M. S. Wong, *Angew. Chem., Int. Ed.*, 1999, **38**, 56.

2 A. Corma, *Chem. Rev.*, 1997, **97**, 2373; M. Eddaoudi, J. Kim, N. Rosi, D. Vodak, J. Wachter, M. O'Keeffe and O. M. Yaghi, *Science*, 2002, **295**, 469; X. Y. Yang, A. Léonard, A. Lemaire, G. Tian and B. L. Su, *Chem. Commun.*, 2011, **47**, 2763.

3 J. Giles, *Nature*, 2004, **427**, 580; O. Bolton and A. J. Matzger, *Angew. Chem. Int. Ed.*, 2011, **50**, 8960; A. T. Nielsen, A. P. Chafin, S. L. Christian, D. W. Moore, M. P. Nadler, R. A. Nissan, D. J. Vanderah, R. D. Gilardi, C. F. George and J. L. Flippen-Anderson, *Tetrahedron*, 1998, **54**, 11793; A. Nielsen, US Patent 5693794 A, 1997;

4 O. Bolton and A. J. Matzger, *Angew. Chem. Int. Ed.*, 2011, **50**, 8960; A. E. D. M. van der Heijden and R. H. B. Bouma, *Cryst. Growth Des.*, 2004, **4**, 999; J. P. Shen, X. H. Duan, Q. P. Luo, Y. Zhou, Q. Bao, Y. J. Ma and C. H. Pei, *Cryst. Growth Des.*, 2011, **11**, 1759.

5 E. Kougoulos, I. Marziano and P.R. Miller, *J. Cryst. Growth*, 2010, **312**, 3509; A.S. Paulino, G. S. Rauber, C. E. M Campos, M. H. Pmaurício, R. R. de Avillez, S. L. Cuffini and S. G. Cardoso, *J. Cryst. Growth*, 2013, **366**, 76.

6 A. Sugawara and T. Kato, *Chem. Commun.*, 2000, 487; G. Xu, N. Yao, I. A. Aksay and J. T. Groves, *J. Am. Chem. Soc.*, 1998, **120**, 11977.

7 G. R. Desiraju, *J. Am. Chem. Soc.*, 2013, **135**, 9952; J. M. Thomas, *Nature*, 1981, **289**, 633; Ö. Almarsson and M. J. Zaworotko, *Chem . Commun.*, 2004, 1889; A. I. Cooper, *Angew. Chem. Int. Ed.*, 2012, **51**, 7892.

8 C. J. Jones, *Chem. Soc. Rev.* 1998, **27**, 289; H. Schönherr, M. W. J. Beulen, J. Bügler, J. Huskens, F. C. J. M. van Veggel, D. N. Reinhoudt and G. Julius Vancso, *J. Am. Chem. Soc.*, 2000, **122**, 4963; Y. Liu, Z. Yang, Y. Chen, Y. Song and N. Shao, *ACS nano*, 2008, **2**, 554.

9 M. Frances Foltz, C. L. Coon, F. Garcia and A. L. Nichois III. *Propellants Explos. Pyrotech.*, 1994, **19**, 133. O. Bolton and A. J. Matzger, *Angew. Chem. Int. Ed.*, 2011, **50**, 8960.

10 J. W. Mullin, *Crystallization,* 4rd ed.; Butterworth-Heinemann: Oxford, Boston, 2001.

11 P. Curie., *Bull. Soc. Franc. Miner.,* 1885, **8**, 145; G. Wulff, Z. Kristallogr. Mineral., 1901, **34**, 449; J. W. Mullin, *Crystallization,* 4rd ed.; Butterworth-Heinemann: Oxford, Boston, 2001; Z. Adam Peng and Xiaogang Peng, *J. Am. Chem. Soc.*, 2001, **123**, 1389.

12 R. Lee Penn and Jillian F. Banfield, *Science*, 1998, **281**, 969; S. R. Challa, A. T. Delariva, T. W. Hansen, S. Helveg, J. Sehested, P. L. Hansen, F. Garzon and A. K. Datye, *J. Am. Chem. Soc.*, 2011, **133**, 20672; C. C. Yec and H. C. Zeng, *J. Mater. Chem. A*, 2014, **2**, 4843.

Physical Chemistry Chemical Physics Accepted Manuscript

 This journal is © The Royal Society of Chemistry 2012